Computer simulation of ionic conduction in ZrF_4-BaF_2 glass

1995 J. Phys.: Condens. Matter 7 8557

(http://iopscience.iop.org/0953-8984/7/45/011)

J. Phys.: Condens. Matter 7 (1995) 8557–8567. Printed in the UK

Computer simulation of ionic conduction in ZrF_4–BaF_2 glass

R Yamamoto, T Kobayashi and Y Kawamoto

Division of Science of Materials, Graduate School of Science and Technology, Kobe University, Kobe 657, Japan

Received 25 May 1995, in final form 12 September 1995

Abstract. Molecular dynamics simulations are performed for a ZrF_4–BaF_2 glass system, which is expected to be a good ion-conducting material, in order to investigate the fundamental conduction dynamics of fluoride ions in the glass. The simulation results show that the ionic conduction is governed by the hopping motion of fluoride ions, with an average hopping distance of 2.5 Å in the glass. This is clearly different from the diffusive motion observed in the melt. It is also found that the mobility is clearly different between bridging (Zr–F–Zr) and non-bridging (Zr–F–(Ba), (Ba)–F–(Ba)) fluoride ions in both glass and melt. The present result gives a satisfactory explanation of two distinct time scales observed in a previous NMR measurement (Y Kawamoto and J Fujiwara 1990 *Phys. Chem. Glasses* **31** 117). The first-passage-time approach is applied to the melt to determine the self-diffusion coefficients of the bridging and the non-bridging fluoride ions separately.

1. Introduction

Since Poulain and co-workers discovered fluorozirconate glasses in 1975 [1], many experimental and simulation studies have been carried out on the structures and properties of these glasses. The static structures of these glasses are rather well understood [2]; it is generally believed that in these glasses ZrF_n polyhedra form a random network by sharing corners and/or edges. However, the relationship between glass properties and their physical origins is not yet understood very well [3]. One of the most interesting findings on the properties of fluorozirconate glasses is that they exhibit notably large electrical conductivity [4, 5] ($\sim 10^{-6}\,\Omega^{-1}\,cm^{-1}$ at 473 K), which is clearly larger than those of other fluoride glasses [6, 7] ($\sim 10^{-10}\,\Omega^{-1}\,cm^{-1}$). Fast-ion-conducting glasses are of considerable technological interest because of their possible applications in batteries [8, 9], sensors [10, 11], and displays [12]. Although the electrical conductivity of these glasses is still smaller than those of crystals which are called superionic conductors, such as PbF_2 ($\sim 10^{-3}\,\Omega^{-1}\,cm^{-1}$ at 473 K), fluorozirconate glasses have attracted considerable attention for the following reasons: (i) fluorozirconate glasses are optically transparent over a wide range of wavelengths; (ii) they can contain a large amount of additives such as rare-earth ions, which are important for applications in active optical devices.

Many studies on fluorozirconate glasses have been carried out to find and design appropriate glass compositions to be used as fast-ion-conducting materials [13–15]. However, only a few studies have been performed to understand the mechanism of ionic conduction based on microscopic considerations [16, 17]. A pioneering simulation study has been made by Angel and co-workers [16]. They performed a molecular dynamics (MD) simulation for a $64ZrF_4{\cdot}36BaF_2$ glass at a temperature of 1200 K. In their simulation, fluoride ions are put into two classes according to the initial ionic configuration of the simulation.

0953-8984/95/458557+11$19.50

Table 1. The potential parameters used in the present simulation.

Ion	z	a (Å)	b (Å)	Reference crystal
F	−1.0	1.500	0.090	ZrF_4
Zr	+4.0	1.380	0.072	ZrF_4
Ba	+2.0	1.800	0.077	BaF_2

These are bridging fluoride ions which have two or more nearest-neighbour zirconium ions (Zr–F–Zr) and non-bridging fluoride ions which have one or no nearest-neighbour zirconium ion (Zr–F–(Ba), (Ba)–F–(Ba)). They then performed an MD simulation and plotted the mean square displacement (MSD) for each class of fluoride ions separately. The length of the simulation is limited to be short enough (~9 ps) so that ions cannot move far away from the initial positions. From the MSD plot, they concluded that the non-bridging ions are more mobile than the bridging ions. Although this conclusion is quite reasonable, it seems rather difficult to reach the conclusion from only a single short simulation run, as they themselves mentioned.

Previously, our group performed a measurement of ^{19}F nuclear magnetic resonance (NMR) for the ZrF_4–BaF_2 glass system, and revealed that the mobility of fluoride ions in the glass has two distinct time scales [3]. A possible way to explain the existence of these two time scales is to accept the argument in [16] of bridging and non-bridging fluoride ions. In this study, we have carried out MD simulations for a $50ZrF_4{\cdot}50BaF_2$ glass at 1000 K (glass) and 4000 K (melt). We have then calculated the self-part of the van Hove correlation function separately for the bridging and non-bridging fluoride ions to find out which contributes more to ionic conduction, and to confirm whether the argument presented in [16] is acceptable.

The self-diffusion coefficient is determined using a recently developed first-passage-time (FPT) approach [18]. This approach makes it possible to distinguish two classes of fluoride ions (bridging and non-bridging) when one calculates the self-diffusion coefficient. In contrast, the MSD approach cannot clearly distinguish them because there is no guarantee that bridging (or non-bridging) ions in a starting configuration remain in the same environment as time goes by.

2. Simulation methodology

2.1. Potential model

MD simulations have been performed for the ZrF_4–BaF_2 glass system in which fluoride ions have large mobility; it is thus expected to be a fast ionic conductor. The simulation system treated in the present study is $50ZrF_4{\cdot}50BaF_2$, since our NMR data are available for the same composition. We used a Born–Mayer (BM) type of interionic potential function without the dispersion term, which is given by

$$U_{ij} = \frac{z_i z_j e^2}{r_{ij}} + f_0(b_i + b_j)\exp\left(\frac{a_i + a_j - r_{ij}}{b_i + b_j}\right) \tag{1}$$

where ze is the ionic charge, a and b are the potential parameters, r_{ij} is the interionic distance between ions i and j, and f_0 ($=6.9511 \times 10^{-11}$ N) is a constant for unit conversion between these terms. The BM-type potential has been successfully used in simulations of various ordered [19] and disordered [20–23] ionic systems. The potential parameters used in this study were determined to give correct structures of reference crystals which contain the same ion species. The parameters are listed in table 1, together with the reference crystals.

2.2. *Simulation details*

Our simulation procedure is as follows.

(i) The simulation is started from a randomly generated initial configuration, and the system is equilibrated at a temperature of 2000 K.

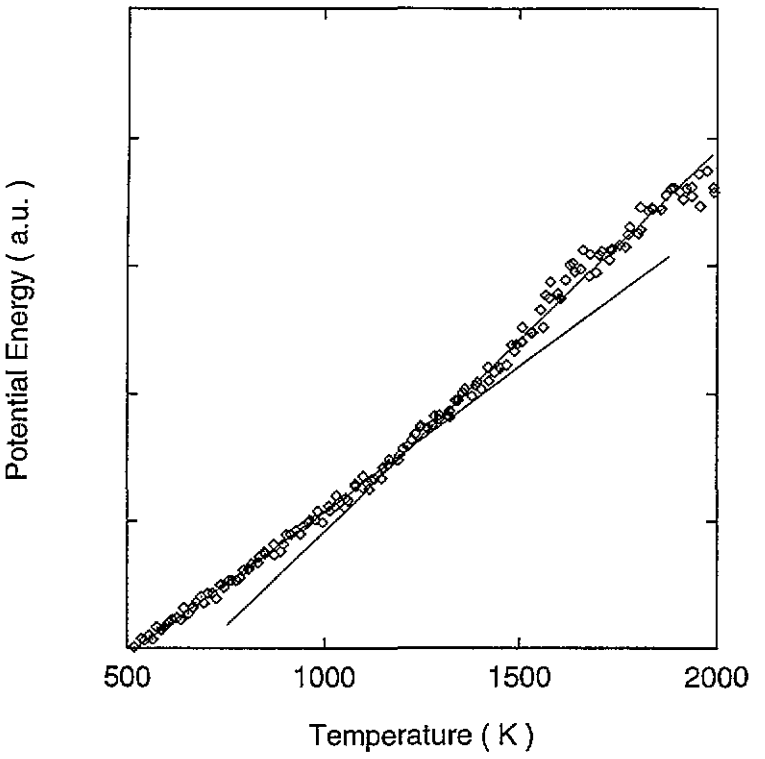

Figure 1. A plot of the total potential energy against temperature during the cooling stage. The glass transition temperature is observed around 1200 K.

(ii) The system is cooled continuously from 2000 K to 300 K. The cooling rate is $-4.0 \times 10^{13}\,\mathrm{K\,s^{-1}}$. Temporal total potential energies of the system are monitored during the cooling stage. These are plotted against temperature in figure 1. This plot has a bend around 1200 K; this represents the glass transition temperature of the model system.

(iii) The annealing run is done at 300 K. The radial distribution function is calculated in this stage. This is shown in figure 2 together with x-ray diffraction data. The agreement of the simulation with the diffraction data is not very good; however one finds that the present simulation can successfully reproduce some important features, such as peak positions, at least qualitatively.

(iv) Two simulation runs are carried out at 1000 K (just below the glass transition temperature, as is seen from figure 1) and 4000 K (melted state) after the system is well equilibrated. The simulation at 1000 K is performed over very long times (~10 ns). We use the microcanonical ensemble (NVE constant) in this stage. To investigate the diffusion mechanism of fluoride ions in the glass, the self-part of the van Hove correlation function

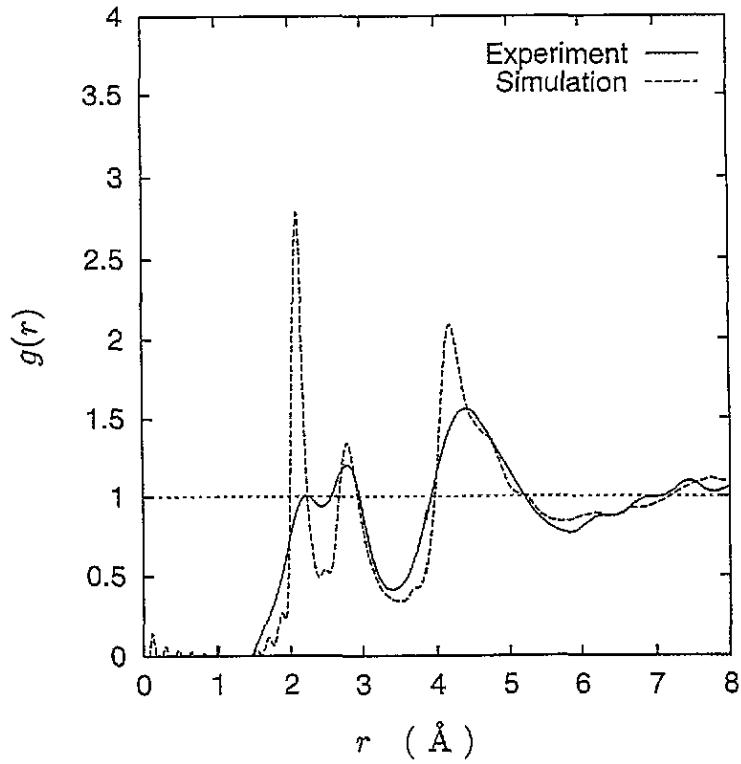

Figure 2. A comparison of the radial distribution function obtained from the present simulation with the x-ray diffraction data.

is calculated, which is defined by

$$G_s(r,t) = \frac{1}{N}\left\langle \sum_{i=1}^{N} \int \delta[r' + r - r_i(t)]\delta[r - r_i(0)]\mathrm{d}r \right\rangle \tag{2}$$

where $4\pi r^2 G_s(r,t)$ represents the distribution of the departure length of ions at the time interval t.

Ewald's summation method was used in all stages of the present simulation to take into account correctly the long-range electrostatic interaction. In stages (i), (ii), and (iii), temperature was controlled using the simple velocity scaling method, and the pressure was kept at 0.1 MPa by adjusting the unit cell length routinely.

3. Results and discussions

The self-part of the van Hove correlation function at a time interval 9 ns, $G_s(r, t = 9\,\mathrm{ns})$, was calculated for fluoride, zirconium, and barium ions in the glass (1000 K). These are shown in figure 3. One finds that only fluoride ions are conductive in the glass, whereas all ions are conductive in the melt (see figure 4). Figure 5 shows $G_s(r, t = 9\,\mathrm{ns})$ for the bridging and the non-bridging fluoride ions in the glass. We used the same method as in [16]

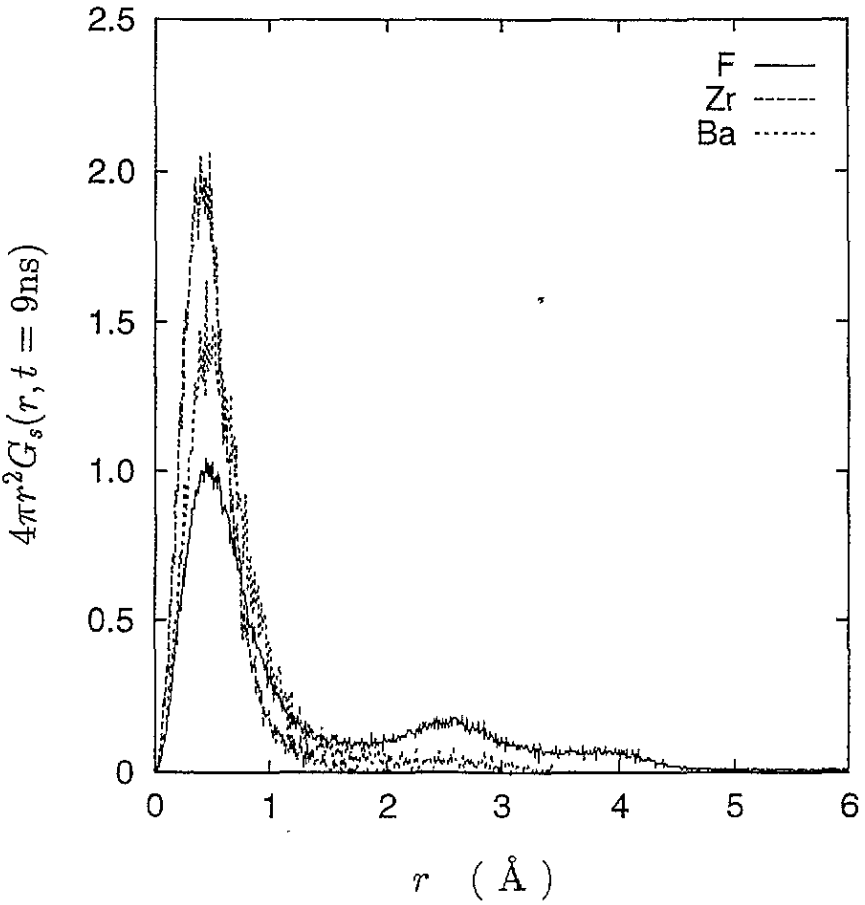

Figure 3. The self-part of the van Hove correlation function for F^-, Zr^{4+}, and Ba^{2+} at 1000 K. This plot shows that only F^- is mobile in the glass.

to distinguish the bridging and non-bridging ions. Cut-off coordination radii are taken to be 2.74 Å for the Zr–F pair and 3.83 Å for the Ba–F pair in the glass. Those in the melt are 3.11 Å for Zr–F and 3.89 Å for Ba–F. These values are the radii where radial distribution functions show the first minimum. The first peaks in figure 5 represent fluoride ions that remain in their initial sites (no hopping). The second and third peaks represent fluoride ions that hopped once or twice within the time interval. One can see that both classes of fluoride ions contribute to the ionic conduction; however, the non-bridging ions are more mobile than the bridging ions. The first moment r_1, which is defined by

$$r_1(t) = \int_0^\infty r 4\pi r^2 G_s(r, t)\mathrm{d}r \Big/ \int_0^\infty 4\pi r^2 G_s(r, t)\mathrm{d}r \tag{3}$$

is calculated and listed in table 2. This measures the average departure length of ions at the time interval t. It is clear from table 2 that the non-bridging ions make a bigger contribution to the ionic conduction than the bridging ions in the glass. The present result supports the argument in [16], and is compatible also with our NMR measurement. It is thus reasonable

Table 2. The first moment r_1 for the glass (1000 K) and the melt (4000 K).

	$r_1(t)$ (Å)	
	Bridging F^-	Non-bridging F^-
1000 K (t = 9 ns)	0.88	1.54
4000 K (t = 125 ps)	3.22	3.44

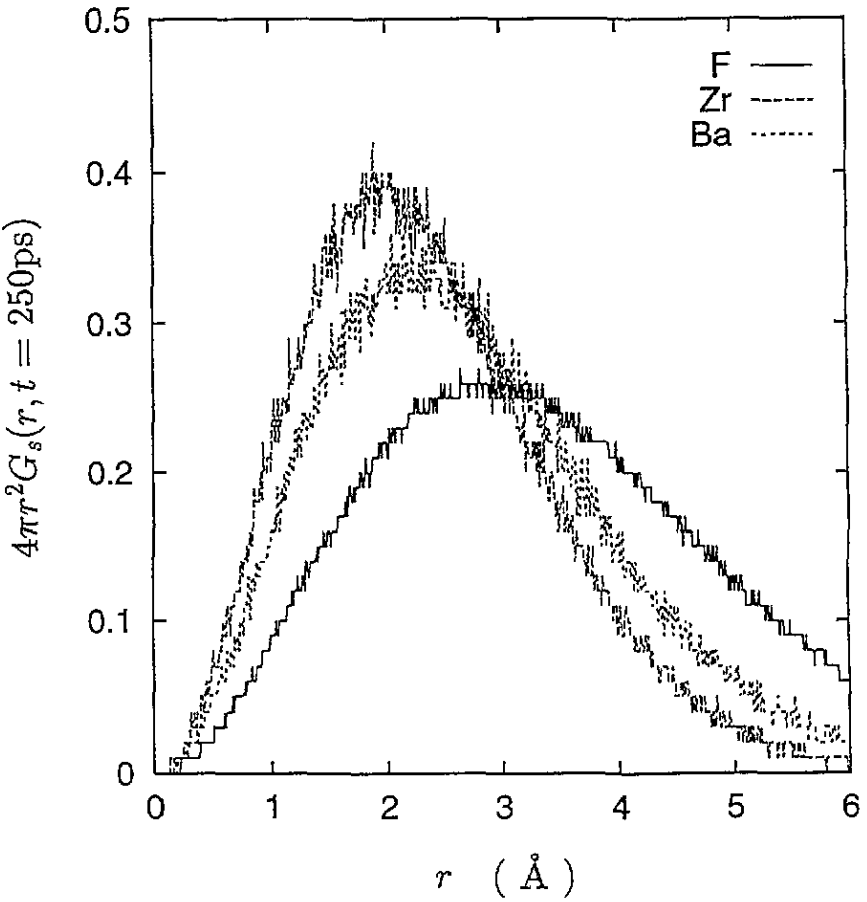

Figure 4. The self-part of the van Hove correlation function for F^-, Zr^{4+}, and Ba^{2+} at 4000K. This plot shows that all ions are mobile in the melt.

to conclude that the origin of two distinct time scales observed in the NMR measurement is attributed to the difference in mobility between the bridging and non-bridging fluoride ions.

The self-part of the van Hove correlation function $G_s(r, t = 250\,\text{ps})$ is calculated also for the melt (4000 K) and shown in figure 6. One finds that the diffusion mechanism in the melt is apparently different from that in the glass (see figure 5). The hopping motion is no longer observed in the melt. The diffusion occurs continuously both in time and space, as is usually observed in simple liquids. By comparing $G_s(r, t = 250\,\text{ps})$ between the two classes of fluoride ions, one finds that the mobility is larger for the non-bridging ions than for the bridging ions in the melt. However, the difference becomes smaller in the melt than

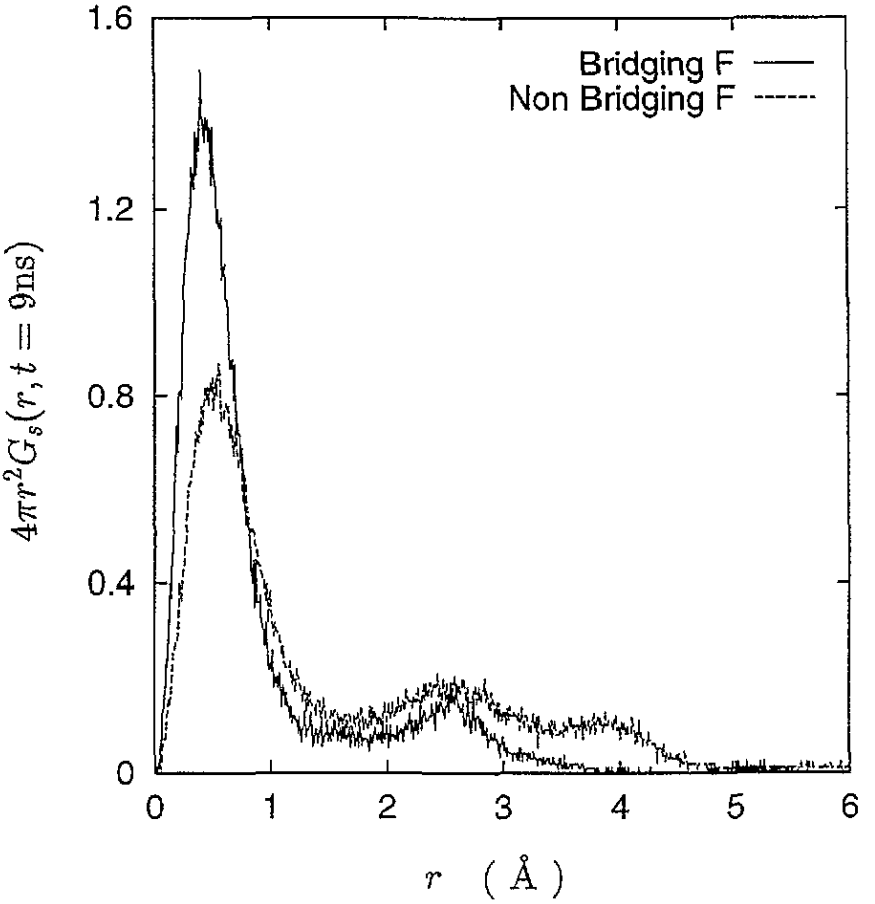

Figure 5. The self-part of the van Hove correlation function for the bridging and non-bridging fluoride ions at 1000 K.

in the glass.

Although the plots of the self-part of the van Hove function give only qualitative information on mobility, one can determine the self-diffusion coefficient by use of the FPT approach [18]. We briefly summarize the FPT approach here. Let us imagine a sphere $S(l; r_0)$ with a radius l centred at r_0. Tracing the trajectory of the particle that is located at r_0 at the time t_0, we record the time $t + t_0$ at which the trajectory crosses the sphere for the first time. The time t is the FPT. We can calculate a histogram of t, which is called the FPT distribution $P_{\text{MD}}(t; l)$, from MD data. By assuming Brownian motion, a theoretical expression for the FPT distribution can be given by

$$P_{\text{th}}(t; l; D) = 2D\left(\frac{\pi}{l}\right)^2 \sum_{n=1}^{\infty} (-1)^{n+1} n^2 \exp\left[-\left(\frac{n\pi}{l}\right)^2 Dt\right] \tag{4}$$

where D is the self-diffusion coefficient. The summation in (4) is truncated at $n = 100$ in our calculations. One can calculate D by comparing $P_{\text{MD}}(t; l)$ with $P_{\text{th}}(t; l; D)$. Since it is possible to evaluate locally defined self-diffusion coefficients by use of the FPT approach, this approach is suitable for the present problem. We have determined the self-diffusion

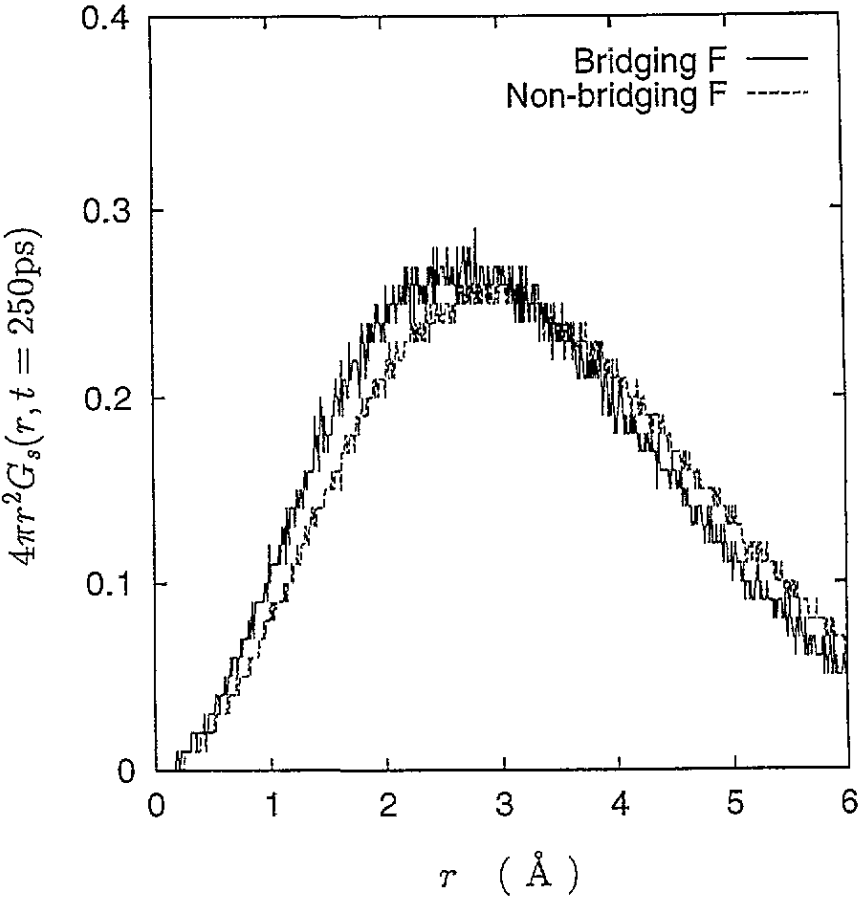

Figure 6. The self-part of the van Hove correlation function for the bridging and non-bridging fluoride ions at 4000 K.

coefficients of the bridging and non-bridging fluoride ions in the melt. The FPT distributions with $l = 3.5$, 5.0, and 7.0 Å are shown in figure 7(*a*), (*b*), and (*c*), respectively. Table 3 summarizes the diffusion coefficients calculated using the FPT approach. One finds that the mobility of the non-bridging fluoride ions is slightly larger than that of the bridging ions even in the melt. We could not accomplish the FPT analysis for the glass, since there were few hopping events even in the present long-time simulation.

Table 3. The self-diffusion coefficients for the melt determined by the first-passage-time approach.

	Self-diffusion coefficient (10^{-4} cm^2 s^{-1})	
l (Å)	Bridging F^-	Non-bridging F^-
3.5	1.23	1.40
5.0	1.32	1.47
7.0	1.34	1.44

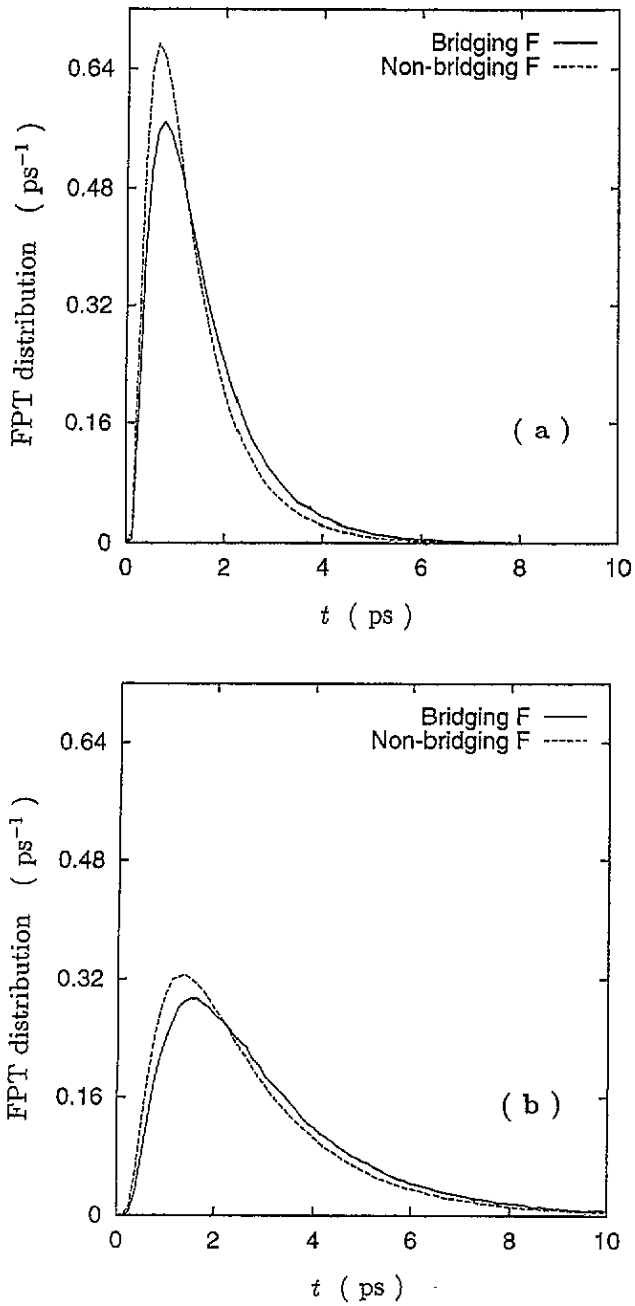

Figure 7. Distributions of the first-passage-time $P_{MD}(t; l)$ for the bridging and non-bridging fluoride ions at 4000 K: (*a*) $l = 3.5$ Å, (*b*) $l = 5.0$ Å, and (*c*) $l = 7.0$ Å.

4. Concluding remarks

We performed MD simulations for a $50ZrF_4{\cdot}50BaF_2$ glass to investigate the fundamental conduction mechanism of ions in the fluorozirconate glasses. We calculated the self-part

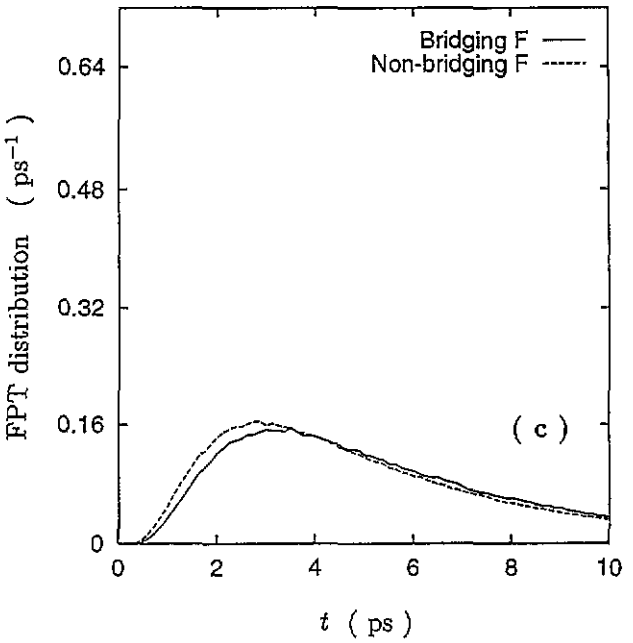

Figure 7. (Continued)

of the van Hove correlation function $G_s(r, t)$ separately for the bridging and non-bridging fluoride ions to study the conduction mechanism from a microscopic point of view. It is found that the ionic conduction is governed by the hopping motion of fluoride ions from one site to neighbouring sites in the glass. The average hopping distance is approximately 2.5 Å for both classes of fluoride ions. In contrast, only diffusive motion is observed in the melt. Comparisons of $G_s(r, t)$ between the bridging and non-bridging fluoride ions showed that these actually have different mobilities; the non-bridging fluoride ions are apparently more mobile than the bridging ions in the glass. It is also found that, in the melt, the mobility is larger for the non-bridging ions than for the bridging ions. However, the difference becomes smaller in the melt than in the glass.

The self-diffusion coefficient was determined for the melt using the FPT approach. This approach makes it possible to evaluate the self-diffusion coefficient separately for the bridging and non-bridging ions. It is found that the self-diffusion coefficient is actually larger for the non-bridging ions than for the bridging ions, even in the melt.

We conclude that the two distinct time scales observed in the NMR measurement can be attributed to the difference in mobility between the bridging and non-bridging fluoride ions. The present conclusion is the same as that of Angel and co-workers [16]; however, we could reach the conclusion more clearly due to the following points. (i) The self-part of the van Hove correlation function provides information on both hopping distances and rates. (ii) When one calculates the self-diffusion coefficient separately for the bridging and non-bridging fluoride ions, the FPT approach is valid even for very long-time simulations, whereas the MSD approach is valid only for short-time simulations in which ions do not depart far from their starting positions.

Acknowledgments

We thank Professor Y Kawamura for providing the original MD code used in the present simulation. The present calculations have been carried out at the Supercomputer Laboratory, Institute for Chemical Research, Kyoto University and the Computer Center of the Institute for Molecular Science, Okazaki, Japan.

References

[1] Poulain M, Poulain M and Lucas J 1975 *Mater. Res. Bull.* **10** 243
[2] Kawamoto Y, Horisaka H, Hirao K and Soga N 1985 *J. Chem. Phys.* **83** 2398
[3] Kawamoto Y and Fujiwara J 1990 *Phys. Chem. Glasses* **31** 117
[4] Leroy D, Lucas J, Poulain M and Ravaine D 1978 *Mater. Res. Bull.* **13** 1125
[5] Ravaine D and Leroy D 1980 *J. Non-Cryst. Solids* **38/39** 575
[6] Petrovskii G T, Leko E K and Mazurin O V 1965 *The Structure of Glass, 4* ed O V Mazurin (New York: Consultants Bureau) p 88
[7] Petrovskii G T 1966 *The Structure of Glass, 6* ed E A Porai-Koshits (New York: Consultants Bureau) p 200
[8] Kennedy J H and Hunter J C 1976 *J. Electrochem. Soc.* **123** 1772
[9] Schooman J 1976 *J. Electrochem. Soc.* **154** 1553
[10] Laroy B C, Lilly A C and Tiller C O 1973 *J. Electrochem. Soc.* **120** 1668
[11] Sher A, Fales C L and Stubblefield J F 1976 *Appl. Phys. Lett.* **28** 676
[12] Rice C E and Bridenbaugh P M 1981 *Appl. Phys. Lett.* **38** 59
[13] Ravaine D, Perera W G and Minier M 1982 *J. Physique Coll.* **43** C9 407
[14] Ravaine D, Perera W G and Poulain M 1983 *Solid State Ion.* **9/10** 631
[15] Kawamoto Y and Nohara I 1987 *Solid State Ion.* **22** 207
Kawamoto Y, Nohara I, Fujiwara J and Umetani Y 1987 *Solid State Ion.* **24** 327
Kawamoto Y, Fujiwara J and Ichimura C 1989 *J. Non-Cryst. Solids* **111** 245
Kawamoto Y, Kanno R and Ichimura C 1990 *J. Non-Cryst. Solids* **124** 271
[16] Angel C A, Cheeseman P A and Tamaddon S 1982 *J. Physique Coll.* **43** C9 381
[17] Inoue H and Yasui I 1987 *Extended Abstract of the 4th Int. Symp. on Halide Glasses* p 106
[18] Munakata T and Kaneko Y 1993 *Phys. Rev.* B **47** 4076
Kaneko Y and Munakata T 1994 *Mol. Simul.* **12** 157
[19] Dixon M and Gillan M J 1978 *J. Phys. C: Solid State Phys.* **11** L165
Gillan M J 1986 *J. Phys. C: Solid State Phys.* **19** 3391, 3517
Walker A B, Dixon M and Gillan M J 1981 *Solid State Ion.* 5 601
Walker J R and Catlow C R A 1981 *J. Phys. C: Solid State Phys.* **14** L979
[20] Sangster M J L and Dixon M 1976 *Adv. Phys.* **25** 247, and references therein
[21] Kinugawa K 1992 *J. Chem. Phys.* **97** 8581
Kinugawa K, Kadono K and Tanaka H 1992 *J. Non-Cryst. Solids* **150** 281
[22] Okazaki S, Miyamoto Y and Okada I 1992 *Phys. Rev.* B **45** 2055
[23] Lantelme F and Turq P 1982 *J. Chem. Phys.* **77** 3177